Photochemistry and Photobiology, 20**, **: *–*

Modulation of Photochemical Damage in Normal and Malignant Cells by Naturally Occurring Compounds†

Yuan-Hao Lee[1], Neeru C. Kumar[2] and Randolph D. Glickman*[1,2,3]

[1]Department of Radiological Sciences, University of Texas Health Science Center, San Antonio, TX
[2]Department of Ophthalmology, University of Texas Health Science Center, San Antonio, TX
[3]Center for Biomedical Neuroscience, University of Texas Health Science Center, San Antonio, TX

Received 29 December 2011, accepted 28 March 2012, DOI: 10.1111/j.1751-1097.2012.01156.x

ABSTRACT

Certain phytochemicals, such as the stilbene, resveratrol (RES, found in red grapes and berries), and the triterpenoid, ursolic acid (UA, found in waxy berries and herbs such as rosemary and oregano), have antioxidant, anti-inflammatory and antiproliferative effects. Two human-derived cell lines, hTERT-RPE with a nonmalignant phenotype derived from retinal pigment epithelium, and ATCC CRL-11147 derived from a malignant skin melanoma, were used as *in vitro* models of photooxidative stress produced by exposure to the broadband output of a 150 W Hg vapor arc lamp at an irradiance of 19–26 mW cm^{-2}. In untreated cells, UV–VIS broadband light exposure produced a loss of proliferative ability, an activation of NF-κB and an increase in protein carbonyl adducts at 24 h postexposure. Pretreatment of the cells with RES or UA at 1–2 μM significantly reduced the amount of phosphorylated NF-κB at 24 h postexposure. RES pretreatment reduced the burden of light-induced protein carbonyl adducts by up to 25% in exposed cells. UA treatment markedly increased the sensitivity of melanoma cells to UV radiation, while conferring some photoprotection to RPE cells. These observations indicate that phytochemicals modulate the cellular response to photochemical stress by interacting with specific cell-signaling pathways.

INTRODUCTION

Light damage to the retina may occur through several well-studied photophysical mechanisms: thermal, mechanical, nonlinear (*i.e.* dielectric breakdown and plasma formation associated with high peak power light pulses) and photochemical processes (1–4). Photochemical damage, because it is most often related to the effects of chronic light exposure and therefore possibly amenable to prevention by external pharmaceutical agents or nutritional factors, will be considered in the present work. Excessive production of reactive oxygen species (ROS) or other free radicals by the absorption of energetic photons in tissue chromophores damages surrounding targets in the immediate cellular vicinity. Accumulation of sufficient cellular damage ultimately leads to visible retinal and retinal pigment epithelial (RPE) lesions. Because of the chronic light irradiation of retina and RPE, photochemical damage has been postulated as a factor contributing to age-related retinal degeneration (5,6). In addition, the use of exogenous antioxidants and free radical scavengers to block or reduce photochemical damage has been extensively studied (7). An important source of protective compounds are phytochemicals naturally occurring in the human diet (sometimes called ''nutraceuticals'') (8). Two compounds, commonly found in human diets and which have been found to confer some protective actions against a variety of oxidative stress mechanisms, are resveratrol (RES) and ursolic acid (UA) (Fig. 1).

RES (see Fig. 1A) is a stilbene phytoalexin, a compound produced by plants in response to stress, such as infections or drought. It is commonly found in grapes, grape extracts and derivative products, such as wine: RES is present in red wine at 0.2–7.0 mg L^{-1} (9,10). Originally thought to be an estrogen agonist because of its structural similarity to estrogen (11,12), additional studies have found either ambiguous effects on the estrogen receptor (13), or variable, concentration-dependent effects (14). Other reported bioeffects of RES have been more consistent, in particular antioxidant, anti-inflammatory, anticoagulative and vasodilatory actions. Due to the oxidation-reduction activity of its hydroxyl substituents, RES can exert direct antioxidant actions. In cardiac tissue, RES quenches ROS (15–17). RES has also been demonstrated to scavenge superoxide anion radicals and directly inhibit lipid peroxidation by scavenging reactive oxygen radical intermediates (15–17). RES may also maintain the concentration of thiol compounds, such as glutathione (18), which serve as substrates for glutathione peroxidases and other antioxidant enzyme systems (19). The antioxidant effects of RES may serve to prevent other chronic conditions, such as cancer. Oxidative damage to DNA is known to produce gene mutations through nucleotide base alterations, chromosome deletions and frame shift errors, thus initiating potentially tumorigenic processes (20,21). By scavenging ROS in the cell, oxidative stress-induced DNA damage is reduced or prevented (22).

UA (Fig. 1A) is a triterpene present, along with many other phytochemicals, in fruits such as privet fruit (*Ligustrum*) and hawthorne fruit (*Cratagegi* sp.), as well as members of various medicinal plants, such as *Rosemarinus officinalis*, *Ocimum sanctum* (and other members of the family Lamiaceae) and

†This invited paper is part of the Symposium-in-Print ''Retinal Photodamage.''
*Corresponding author email: glickman@uthscsa.edu (Randolph D. Glickman)

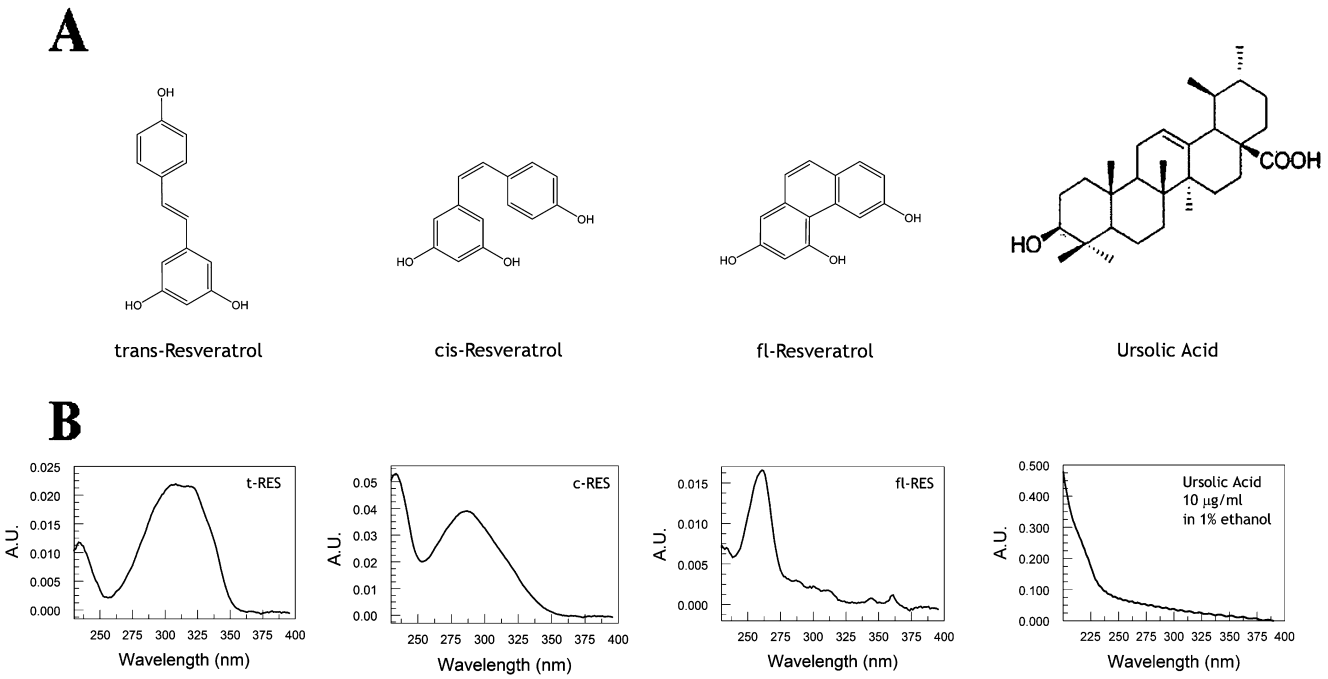

Figure 1. Molecular structures of the compounds used in this study. (A) From left to right: *trans*-RES (the native form), *cis*-RES (the photoinduced isomer), fl-RES (a highly fluorescent photoderivative; the structure shown here is that proposed by Galeano-Diaz *et al.* [42]) and ursolic acid. (B) The UV absorption spectra of each of the above compounds; from left to right: t-RES, c-RES, fl-RES and ursolic acid. The absorption spectra of t-RES, c-RES and fl-RES were obtained from the photodiode array detector during the separation of the samples shown in Fig. 3. The absorption spectrum of ursolic acid, 10 μg mL^{-1}, was obtained by standard spectrophotometry using a Shimadzu Pharmaspec UV-1700. The ursolic acid sample was prepared by dilution in distilled water of a 1 mg mL^{-1} ethanolic stock solution (1% residual ethanol).

Eugenia jumbolana. These plants have been used since ancient times in several traditional medicine pharmacopeias, *e.g.* Greek and Chinese, to alleviate inflammatory conditions and reduce hypertension (23,24). UA is reported to have a wide range of actions in cells and tissues. In a study utilizing as an endpoint the metabolism of arachidonic acid by murine macrophages, human platelets and HL60 leukemic cells, UA was found to inhibit the activity of lipoxygenase in the cells, thus reducing the production of leukotrienes (24). In that same study, cellular toxicity of UA was low; only at a concentration of 100 μM was a loss of cellular viability observed. UA appears to be especially active in the cellular environment; although UA was relatively ineffective in scavenging superoxide anion in a cell-free system, it was a very effective scavenger in a system containing human neutrophils stimulated into a respiratory burst by treatment with zymosan A (23). In contrast, in different cell-free systems of lipid peroxidation and superoxide anion production, UA was found to have a similar level of antioxidant activity as α-tocopherol (25), and was generally effective in preventing lipid peroxidation in an *in vitro* model utilizing isolated rat liver microsomes (26). UA also inhibits NF-κB activation at multiple sites in this transcription factor's pathway, including its phosphorylation and ability of p50/p65 to bind to DNA (27). NF-κB is an important transcription factor responding to a variety of external stressors, such as toxins, pathogens, ischemia, shear stress and radiation-induced oxidative stress (28–30). Photooxidative stress induced in cells and tissues by light (UV and VIS) and laser exposures also activates NF-κB (31–33); the transcription factor is regarded as an important biomarker in photobiology (34). Through the modulation of this transcription factor, UA reduces inflammation not only by lowering the activity of proinflammatory enzymes such as cyclooxygenase-2 (COX-2) and matrix metalloproteinase-9, but also by exerting an antiproliferative effect, thus conceivably conferring an anticancer action. Indeed, UA has been demonstrated to have antiproliferative effects on several cervical cancer cell lines (HeLa, CaSki and SiHa) (35,36). In mouse models of skin cancer, a topical application of UA reduced the number of skin cancers, and lowered the activity of several proinflammatory markers, produced by the application of several tumor promoters and inflammatory agents (37,38). UA-supplemented chow inhibited the growth of exogenous human mammary tumors in a mouse model (39). Thus, UA exerts anticancer activity in both *in vitro* and *in vivo* models.

Although UA itself has no strong chromophore in the UV or VIS bands, RES is highly optically active (the optical absorption spectra of these compounds are shown in Fig. 1). UV and VIS light in the range of 254–550 nm will photoisomerize trans-RES (t-RES) to cis-RES (c-RES), as reported by Trela and Waterhouse (40) and confirmed in our own laboratory (unpublished observations), yet there are few reports on the bioeffects of the cis isomer (41). Moreover, the photoisomerization of t-RES to c-RES is not the only light-sensitive reaction. Continued exposure of c-RES to UVA produces an irreversible conversion to a tricyclic, phenanthrene-like compound, fl-RES, that is highly fluorescent (42) (Fig. 1A). We have confirmed the existence of this photoderivitization reaction, as well as the highly fluorescent nature of the resulting product, and report here that this derivative is

capable of photosensitizing proteins in RPE and presumably retinal cells. We have also studied the ability of RES and UA to modulate the response of normal and cancer cells to photochemical stress. In our previous work, we demonstrated that exposing the cells to short-wavelength visible light, *e.g.* the 488 and 514.5 nm mixed output of an Argon laser, at an irradiance of 10–20 mW cm^{-2} and an exposure duration of 5–10 min, produced photooxidative stress in the cells, as indicated by fatty acid peroxidation (43), protein carbonyl adducts (3) and NF-κB nuclear translocation (33). In the present work, two *in vitro* models, a well-characterized RPE cell line and a standardized human skin melanoma (SM) cell line, were used to test the antioxidant effects of RES, its photoderivatives and UA.

MATERIALS AND METHODS

Cell lines. Experiments were conducted with the p53-reactive hTERT-RPE (human retinal pigment epithelium) cell line (44) and the CRL-11147 human SM cell line (ATCC, Manassus, VA). Cells were grown in standard culture conditions in DMEM/F-12 and DMEM, respectively, with 10% fetal calf serum. Both media were supplemented with gentamycin (5 μg mL^{-1}), penicillin (100 IU mL^{-1}), streptomycin (100 μg mL^{-1}) and amphotericin B (250 ng mL^{-1}) (all supplied by Cellgro, Manassas, VA). The studies were designed to measure radiation-induced oxidative stress and DNA damage in relation to the antioxidant effect of UA.

Reagents. RES, >98% pure, from *Polygonum* root was obtained from MP Bio (Solon, OH). UA, >90% pure, from cranberries was obtained from Sigma-Aldrich (St. Louis, MO). The structures of RES (MW 228.24), its isomer and photoderivative, as well as that of UA (MW 456.70), are shown in Fig. 1A. The structure of fl-RES is that proposed by Galeano-Diaz *et al*. (42).

A stock solution of RES was prepared at a concentration of 1 mg mL^{-1} in ethanol and stored at −20°C. The UA stock solution was prepared in ethanol or in DMSO (in different experiments) at a concentration of 1.7 mg mL^{-1} and stored at 4°C. Analysis by HPLC indicated that these stock solutions were stable under these storage conditions for at least 4 months. For use, the stock solutions were diluted in cell culture medium to working concentrations of 0.1–8.0 μM or as otherwise specified. The residual solvent (ethanol or DMSO) in the culture media was 0.8% or less, depending on the working concentration of the study compound. For the HPLC measurements, chromatography grade acetic acid and methanol were obtained from EMD (Gibbstown, NJ) and acetonitrile from Sigma-Aldrich.

Treatment and irradiation of cells. Cells were exposed to the broadband output (containing UVA, UVB and VIS spectra) of a 150 W Schoeffel Instruments Hg vapor arc lamp for a specified period of time. Two lamp configurations, which produced different irradiances, were used to accommodate different cell culture formats. For cells growing in standard 24- or 96-well plates or 100-mm Petri dishes, the exposure irradiance was 19 mW cm^{-2}. For cells growing in 6-cm Petri dishes, the exposure irradiance was 26.7 mW cm^{-2}. Two exposure protocols were used: (1) For the experiments in which p65-P and p53 were measured by immunoprecipitation and Western blot techniques, the cells were grown until they were fully attached, pretreated with either RES or UA for durations ranging from 1 to 8 h, and then the treatment was terminated by media replacement (*i.e.* no phytochemical was present) prior to irradiation. Cells were exposed for 10 min to the Hg vapor arc lamp at an irradiance of 26.7 mW cm^{-2}, in the complete growth medium, including phenol red indicator. (2) For the experiments in which NF-κB (p65-P) was measured by ELISA, cells were plated in 100-mm diameter Petri dishes and allowed to grow to confluence. Prior to light exposure, the standard culture medium was replaced with phenol indicator-free medium containing the phytochemical, either RES or UA at the desired concentration, and the cells were incubated at 37°C for 1 h. Following this treatment period, the culture dishes containing the cells were exposed to the output of the Hg vapor arc lamp at an irradiance of 19 mW cm^{-2} for 7.5 min. Sham controls were placed on the laboratory bench under normal ambient laboratory light for the same period of time. Following exposure, the cells were returned to the incubator for 1 or 24 h, without changing the culture medium. At the end of the incubation period, NF-κB was assayed by ELISA as described below.

Measurement of p65 and p53 in cell extracts by immunoprecipitation and Western blot. Following irradiation, the cells were returned to normal growth medium, incubated for 4 h and harvested for protein extraction. For the extraction of nuclear proteins, cell pellets were processed according to published methods (45). For whole protein extraction, modified RIPA buffer (50 mM Tris, pH 7.2, 150 mM NaCl, 1% NP-40, 1% sodium deoxycholate, 0.1% SDS and 2 mM EDTA) with protease inhibitor cocktail was used. Protein concentration was determined using the bicinchoninic acid (BCA; Pierce) assay. Immunoprecipitation was conducted with at least 100 μg total protein (input) to conjugate with an antibody raised against the phosphorylated NF-κB p65 (p65-P) component (cat. no. SC-33039; Santa Cruz Biotechnology, Santa Cruz, CA) and an anti-p53 antibody (cat. no. P6749; Sigma-Aldrich) followed by incubation using agarose beads (cat. no. SC-2003; Santa Cruz Biotechnology). Heat denaturation at 95°C for 10 min was performed before the separation of protein extracts on a 12% SDS gel (0.37 M, pH 8.8 Tris, 12% acrylamide/Bis 29:1, 0.1% SDS, 0.5 mg mL^{-1} and 0.05% TEMED) with a 4% stacking gel (0.12 M, pH 6.8 Tris, 3.9% acrylamide/Bis 29:1, 0.1% SDS, 0.5 mg mL^{-1} and 0.1% TEMED). During electrophoresis, the current in the SDS running buffer (0.025 M Tris base and 0.19 M glycine) was set to 80 mA for up to 2 h; for gel transfer, the voltage in the transfer buffer (0.025 M Tris base, 0.19 M glycine, 0.05% SDS and 4% methanol) was set to 22 V overnight, with cooling applied to the transfer apparatus. These data are reported in Fig. 10A,B.

Measurement of NF-κB in RPE cells by ELISA. In some experiments, the activation of NF-κB was assessed by determining the level of p65-P in cytosolic lysates using an ELISA, following treatment with RES and UA prior to light exposure, as described above. In these experiments, RES and UA were tested over a concentration range of 0.1–2.0 μM. After the light exposure, the cells were incubated at 37°C for either 1 or 24 h, harvested from the Petri dishes, lysed and probed for NF-κB activation using a commercial ELISA kit selective for the phosphorylated p65 component (p65-P) of NF-κB (Cell Signaling Technologies, Danvers, MA), according to the manufacturer's protocol. These data are reported in Fig. 4A,B.

Photoderivitization of RES. A RES solution (10 μg mL^{-1} in ethanol) was exposed to the output of the 150 W Hg arc lamp at an irradiance of 19 mW cm^{-2} for 20 min. This solution was freely open to the atmosphere during the light exposure. Aliquots from this stock were taken and diluted for use in the cell culture experiments.

Apoptosis assay. Cellular apoptosis was assayed at 4 h postirradiation with the fluorochrome YO-PRO-1 and red PI (propidium iodide), contained in the Vybrant Apoptosis Assay Kit #4 (Molecular Probes/Invitrogen-Life Technologies). The manufacturer's protocol was followed for processing the cells and then the cells were observed with a fluorescence microscope. Necrotic cells initially admit only PI (giving red fluorescence), but exclude YO-PRO-1. Apoptotic cells, in contrast, admit only YO-PRO-1 (giving green fluorescence). Eventually, dead cells may admit both probes and fluoresce yellow. Apoptotic cells were identified by the presence of the green fluorescence of YO-PRO-1 alone, and necrotic cells by the presence of PI alone. Cell counting was performed in triplicate with randomly chosen fields for determining apoptosis indices.

High performance liquid chromatography. Separation of RES isomers and its photoderivative: Separations were carried out at RT using a Waters μBondapak-C18 column (150 × 3.9 mm) and a mobile phase consisting of 25% methanol/10% acetonitrile/1% acetic acid in water, at a flow rate of 0.5 mL min^{-1}. Twenty microliter aliquots were used for the analysis. The RES isomers t-RES and c-RES are moderately fluorescent, whereas fl-RES is highly fluorescent; however, of all of these compounds, t-RES has the strongest absorption in the UV, with a broad absorption peak in the range of 300–310 nm, as shown in Fig. 1A (40). Therefore, tandem UV detection at 306 nm and fluorescence detection with λ_{Ex} = 315 nm and λ_{Em} = 382 nm were employed to discriminate the RES isomers and the fluorescent photoderivative.

Assessment of cellular oxidative stress using 2′,7′-dichlorodihydrofluorescein (DCFH): Esterified DCFH diacetate stock solution (Molecular Probes/Invitrogen-Life Technologies) was prepared as 0.5 mg mL^{-1} in methanol and stored at −20°C. The working dilution of 10 μM DCFH was made in complete culture media shortly before its use in the experimental protocol; the media containing the DCFH was kept in a light-tight container until it was added to the culture plates. After 24 h of UA treatment, 10 μM DCFH diacetate was administered to cells 1 h prior to irradiation. Intact suspended and attached cells were collected immediately after irradiation. Extraction of probes from the cells and HPLC analysis of oxidized DCFH were performed as previously described (46). Briefly, under the Phillips F32T8 fluorescent laboratory lighting shielded by yellow (550 nm cut-on longpass) filters, the cell lysates were extracted on Waters Oasis HLB solid-phase extraction cartridges using methanol as the elution solvent. The eluates were dried and resuspended in mobile phase (8 mM ammonium phosphate, pH 8.0, in 60% methanol). The HPLC analysis was carried out on a 3.9 mm × 300 mm Phenomenex Bondclone-C_{18} column, at a flow rate of 1 mL min^{-1}. Twenty microliters aliquots were injected into the column and separations were carried out at RT. Fluorescence detection parameters were λ_{Ex} = 488 nm and λ_{Em} = 530 nm.

Protein carbonyl assay. Carbonyl adducts produced by oxidative stress to proteins were assessed at 24 h following a 10 min exposure of RPE cells to the Hg arc lamp at 19 mW cm^{-2}, as described above. The effects of a 1 h pretreatment with t-RES or fl-RES on protein oxidation were tested by adding these compounds to the growth media. A dilution of a stock solution of t-RES was added, so the final concentration in the growth media was 10 μM. The fl-RES was prepared by photoderivitization of t-RES, as described above. The precise concentration of fl-RES was not known exactly, but an amount of the fl-RES material was added to the growth media to achieve a 1:10 dilution of the original stock. Measurement of carbonyl adducts was carried out with the Oxyblot assay (Chemicon/Millipore, Billerica, MA), following the manufacturer's protocol. In the Oxyblot assay, RPE cells were lysed and the soluble proteins reacted with dinitrophenylhydrazine to derivatize the adducts, which were then separated using polyacrylamide gel electrophoresis, followed by Western blots using a chemiluminescence-linked antibody (supplied in the Oxyblot kit) to detect the derivatives. The intensity of the resulting images of the luminescent transfers was measured and analyzed using the Image Pro software package (Media Cybernetics, Bethesda, MD). By taking a linear measurement of the pixel intensity along the length of the gel image, and then integrating the area under that curve, a quantitative measure of the relative, total protein carbonyl content of the retinal proteins was obtained for each experimental condition. Additional details on this analytical technique have been previously reported (47).

BrdU staining. RPE cells were plated to about 50% confluency in Chamber Slides (Nalge Nunc International). After 24 h of UA treatment, all cell culture media were replaced by fresh media containing 10 μM BrdU. Cell fixation was performed with 70% ethanol followed by washing and incubation with anti-BrdU antibody and secondary fluorescein antibody, sequentially. Hoechst 33342 (10 μM) was applied for 2 min before microscopic observation, in order to stain all cell nuclei present in the field.

Statistical analysis. All data were normalized relative to the corresponding internal control. Error bars were drawn based on the ranges of disparity (in cases of n = 2) or the standard deviation values (in cases of n > 2). Other statistical tests, specifically ANOVA followed by the Bonferroni multiple comparison tests, were carried out using the ProStat statistical software (Polysoftware, Pearl River, NY).

RESULTS

RES and its photoderivatives

The ability of UVA and short wavelength VIS light to photoderivatize RES was confirmed. Excitation–emission scans were made to characterize the fluorescent properties of the derivatives (Fig. 2). Following exposure to the Hg vapor arc lamp, a fluorescent derivative, designated fl-RES, appeared with an excitation peak at 315 nm, and a triphasic emission curve, with peaks at 360, 380 and 405 nm, likely corresponding to the three rings of the tricyclic Fl-RES, which is the proposed structure of this photoderivative (42). Longer duration light exposures increased the yield of Fl-RES (Fig. 2).

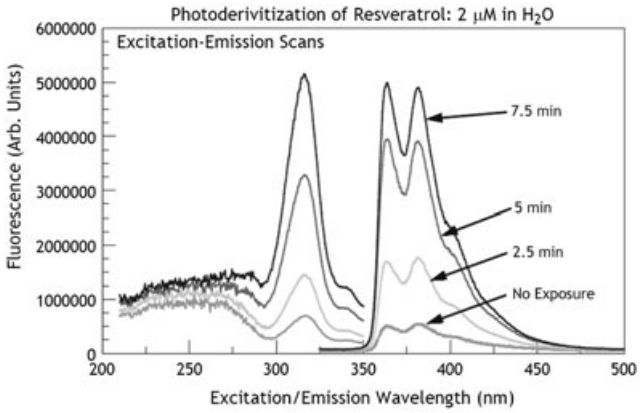

Figure 2. A family of fluorescence excitation–emission curves, showing the increasing yield of the fluorescent derivative of RES (Fl-RES), proportional to the duration of light exposure. A 1 mM stock solution of native RES, *i.e.* the trans isomer, was made in ethanol. Two milliliters of this solution was placed in a quartz spectrophotometer cuvette, and irradiated with a Hg vapor arc lamp at 19 mW cm^{-2} for various times up to 7.5 min. After each exposure time was completed, an aliquot was taken, diluted to a working concentration of 2 μM in distilled water, and placed in a spectrofluorimeter to measure its excitation–emission curve. Note the excitation peak at 315 nm, and emission peaks at 360, 380 and 405 nm. Spectra were recorded in a Jobin-Yvon-Spex Fluorolog-3 spectrofluorimeter.

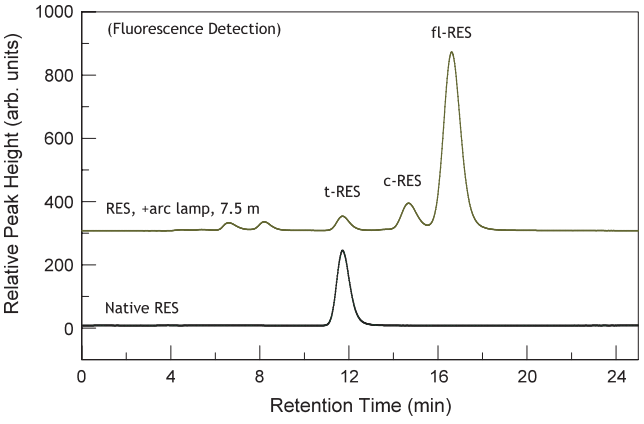

Figure 3. HPLC analysis of RES and its photoproducts. Lower trace: native trans-RES (in the dark). Upper trace: photoproducts formed by RES exposure to Hg arc lamp at 19 mW cm^{-2} for 20 min. Detection of all compounds was by fluorescence detection with λ_{Ex} = 315 nm and λ_{Em} = 382 nm. Small peaks at 6.5 and 8 min were not identified. Other chromatographic details are given in the Materials and Methods section. The UV spectra of the major peaks (t-RES, c-RES and fl-RES) were obtained with a PDA detector placed in tandem with the fluorescence detector, and are shown in Fig. 1.

These photoproducts were separated using HPLC (Fig. 3). After 20 min of exposure to the Hg arc lamp (19 mW cm^{-2}), a 10 μg mL^{-1} solution of RES (100% in the form of t-RES) was reduced to 0.85 μg mL^{-1} t-RES (>90% loss), due to the conversion to c-RES (peak with RT ≈ 14.5 min, upper trace

in Fig. 3) and fl-RES (peak with RT ≈ 17 min, upper trace in Fig. 3). Although t-RES and c-RES are somewhat fluorescent, the fl-RES derivative is highly fluorescent (the peak shown in the figure could not be precisely quantitated, due to lack of an appropriate standard). The fl-RES prepared in this way was used in the subsequent studies of its biological activity.

Modulation of photooxidative stress responses in RPE cells by RES and UA

The bioeffects of RES isomers and UA were investigated in the hTERT-RPE cell line, using NF-κB as a biomarker of oxidative stress induced by broadband light exposure (conditions given in the Materials and Methods section). Results of these experiments indicated that both RES and UA treatment, at a concentration of 1–2 μM, significantly reduced at 24 h postexposure, but not at 1 h, the levels of activated NF-κB ($P < 0.05$ for RES effect and $P < 0.002$ for the UA effect), compared with untreated cells (Fig. 4). We speculate that the RES effect was not observed at 1 h postexposure because the p65 was derived at that early time point from cytosolic stores, whereas at the 24 h time point newly synthesized protein was being utilized, which may have been more sensitive to upstream effects of RES treatment on cell-signaling pathways.

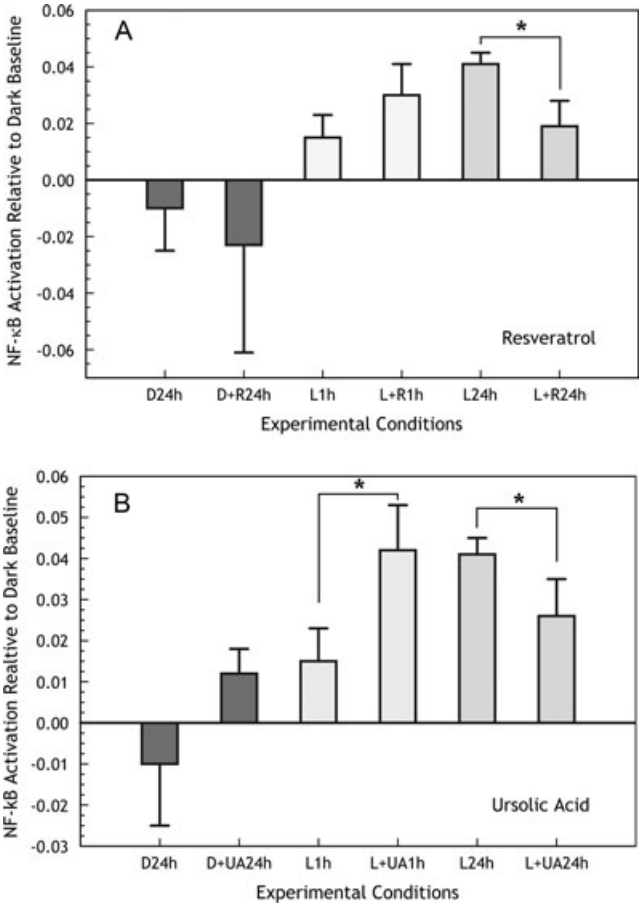

Figure 4. Broadband light exposure causes activation of NF-κB in RPE cells. The phosphorylation of p65 was measured in the cells using ELISA. (A) Treatment of the RPE cells, starting at 1 h before the light exposure, with t-RES at 2 μM reduced NF-κB activation in these cells at 24 h, but not at 1 h, after exposure to the Hg vapor arc lamp for 7.5 min at an irradiance of 19 mW cm^{-2}, compared with untreated cells. The difference in the NF-κB activation in treated and untreated RPE cells at 24 h postexposure was significant ($n = 4$; $P < .05$, Bonferroni multiple comparison test). (B) Treatment of the RPE cells with UA reduced NF-κB activation in light-exposed RPE cells. Arc lamp exposure conditions were as described above. Cells were treated, starting at 1 h before light exposure, with 2 μM UA, and p65-P was measured in the cells a 1 and 24 h postexposure. UA treatment did not reduce NF-κB activation at 1 h; in fact it was significantly elevated, but a significant reduction in the phosphorylated transcription factor was found at 24 h, compared with the untreated cells ($n = 4$; $P \sim 0.002$, Bonferroni multiple comparison).

Bioeffects of Fl-RES

Considering the strong fluorescence of fl-RES, the possibility existed that this photoderivative of RES could function as a photosensitizer. To address this question, cultures of hTERT-RPE cells were pretreated with RES (10 μM) or fl-RES (concentration not quantified, but the material was prepared as described in the Materials and Methods section) for 1 h and then exposed to light from the Hg arc lamp for 10 min at an irradiance of 19 mW cm^{-1}. After the light exposure, the cells were incubated for 24 h, harvested, and the relative levels of protein carbonyl adducts were determined in the samples using the Oxyblot assay. Broadband light exposure increased the overall protein carbonyl content of virtually all RPE cell proteins by 15.4% (Table 1 and Fig. 5A). RES pretreatment lowered the light-induced carbonylation of most RPE cell proteins; in fact, the overall carbonyl load in light-exposed RPE cells, pretreated with RES, was reduced by 9.7% compared with the nonexposed cells and was about 25% lower than in the light-exposed cells (Fig. 5A and Table 1). In contrast, fl-RES appeared to have a pronounced photosensitizing effect, increasing light-induced protein oxidation in the RPE cells by 70.5% compared with the nonexposed control cells (Fig. 5B). These results are summarized in Table 1.

Differential effects of UA on photooxidative stress responses in normal and tumor cells

The results described above, showing UA modulation of NF-κB activation, following photooxidative insult, suggested that this phytochemical may have broader effects, such as on inflammatory responses and cell cycle propagation. In addition to the hTERT-RPE cell line, UA effects were also investigated in an SM cell line. After the administration of a subcytotoxic dose of UA (< 10 μM), the cellular content of ROS, as measured by DCFH oxidation, was unexpectedly increased in both RPE and SM cell lines. The elevated DCFH oxidation, however, was more marked in RPE cells than in the SM cells (Fig. 6). Nevertheless, the UA-induced elevation in ROS did not reduce cell viability as assessed by the MTT assay (data not shown). Although the variability in the data in these measurements was rather high, the overall trend indicated that, when combined with UV irradiation, the UA-induced ROS was reduced in RPE cells but increased in SM cells (Fig. 6, compare "UA + L" with "L"). This finding suggests that UA pretreatment specifically potentiates the radiation effect in SM cells leading to a disparity of cellular ROS between RPE and SM cells, at least in the early responses to the radiation. This

Table 1. Integrated values of gel density scans from the Oxyblot assay of protein carbonyl adducts in RPE cells treated with t-RES or fl-RES and then exposed to the broadband output of the Hg vapor arc lamp for 10 min at an irradiance of 19 mW cm^{-2}.

Pretreatment	Control (no light or pretreatment)	Light only	% Difference from control	Light + pretreatment	% Difference from control
t-RES	233.3 ± 21.1	272.2 ± 4.0	15.4	211.8 ± 12.8	−9.7
fl-RES	278.0 ± 11.6	407.1 ± 27.1	37.7	580.7 ± 57.6	70.5

Values represent the means and ranges from two assays. Note that these values are integrals and thus are unitless. Percent differences between values are calculated as $[V_1 - V_2/((V_1 + V_2)/2)] \times 100$, where V_n represents an experimental value.

hypothesis received some support by the observation that the radiation killing effect on SM cells was preferentially enhanced by UA pretreatment at 24 h post exposure to UV–VIS light (Fig. 7). These results imply that UA exerts distinct actions in healthy and tumor cells.

The time course of apoptosis following UA treatment and UV exposure was evaluated in SM cells using the Vybrant Live/Dead assay. Cells were observed microscopically and live, necrotic and apoptotic cells were counted in each microscopic field. The results of these studies indicated that radiation-induced cell death was facilitated by UA pretreatment, particularly in the SM cells, as shown by the drop in the number of SM cells per microscope filed as early as 8 h postirradiation (Fig. 8). The proportion of cells dying through apoptosis increased in the UA-plus-radiation treated SM cells throughout the 24 h monitoring period (Fig. 9). This result suggests differential modulatory functions of UA on cell death and apoptosis in RPE and SM cells. Studying cell cycle arrest with BrdU staining indicated that UA blocks the cell cycle rather than directly initiating apoptosis in RPE cells (data not shown, but confirmed by flow cytometry, which showed that UA treatment causes a majority of RPE cells to remain in G1 phase). This finding was in contrast to the effect of UA on SM cells, in which the treatment of 1 μg mL^{-1} (2.2 μM) UA reduced DNA synthetic activity to about 50% of the basal rate. This finding indicates the potential involvement of p53, which dominates both cell cycle regulation and apoptosis, in mediating the mechanism of action of UA. This hypothesis was supported by the following observation that UA increased the expression of p53 in SM cells.

By using anti-p53 and anti-p65-P antibodies in both immunoprecipitation and immunoblotting studies, the specific action of UA on p53 regulation and NF-κB activation was evaluated following UV–VIS irradiation (Fig. 10). The level of p65-P was decreased by UA treatment in SM cells (compare, in Fig. 10A, the "UA" treatment group with "Control" for SM cells) whereas the level of p53 was increased in the total protein fraction (Fig. 10B, compare the "Control" *vs* "UA" groups). In contrast, UA treatment had little effect on the basal level of p65 phosphorylation (Fig. 10A) and p53 expression in RPE cells (Fig. 10B). With respect to the cellular response to UV–VIS radiation, pretreatment with UA restored the activation of NF-κB inhibited by UV radiation in SM cells, rendering it similar to the NF-κB response in the normal, RPE cells (Fig. 10A, compare the "UA-L" and "L" groups), and reduced the radiation-induced p53 upregulation in RPE cells while maintaining a strong p53 response in SM cells. These results reveal the ability of UA to modulate cellular signaling in response to radiation insult. Along with the result shown in the apoptosis assay, the distinct regulatory effects of UA on p53 protein expression may contribute to the relative photoprotection of normal cells, while enhancing the cytotoxic effect of the UV–VIS radiation on tumor cells.

DISCUSSION

Differential effects of RES and UA in normal and malignant cells exposed to photooxidative stress

Although in the adult, phakic eye, retina and RPE cells are not normally exposed to UV light, they are irradiated by wavelengths as short as 360 nm, which transmitted through the ocular cornea and lens are capable of inducing photochemical damage. This topic has been recently reviewed (47). Moreover, in the juvenile eye, before the physiological lens has begun its yellowing process, the retina and RPE are subject to UVB light damage (48). Therefore, although normally situated in very different bodily locations, both RPE and skin cells—at some point in or throughout their life—receive UV and VIS irradiation, and it is reasonable to compare the photodamage mechanisms in these different cell types. A major observation in the present work is that two phytochemicals, RES and UA, exert general antioxidant effects in cells subjected to photooxidative stress, *i.e.* exposure to broadband light containing radiation in the UVB, UVA and VIS bands. In the case of RES, this is not a surprising finding, because of the well-documented antioxidant properties of the compound. The prooxidant property of fl-RES, the photoderivative of RES, is a new finding, and is discussed in detail below. UA, based on its structure, does not possess any obvious substituent capable of supporting redox reactions, and thus its effects may be the result of interactions with specific cell-signaling pathways. A surprising observation made in the present study is that UA may have different actions in normal and malignant cells. In the nonmalignant RPE cells, UA increased the content of ROS, as measured by DCFH oxidation, whereas this effect was less apparent in the SM cancer cells (Fig. 6). In the present data set, the effect of UA on the cellular oxidative state is not entirely established; however, the trend in the data suggests that there is a difference. The import of such a difference in the intracellular redox state is not entirely clear at this time; we found that the RPE cells were not adversely affected by the increased ROS content, as evidenced by their continued growth and viability. On the other hand, UA treatment markedly sensitized the SM cells to the UV–VIS exposure; the early cell mortality was greatly increased in the SM cells treated with UA (Fig. 8). The response of the RPE cells to the UV–VIS irradiation was not noticeably affected by UA treatment. This differential effect of UA appears to be due

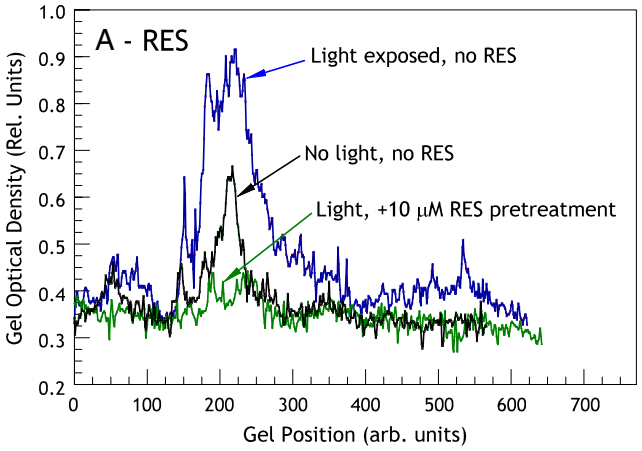

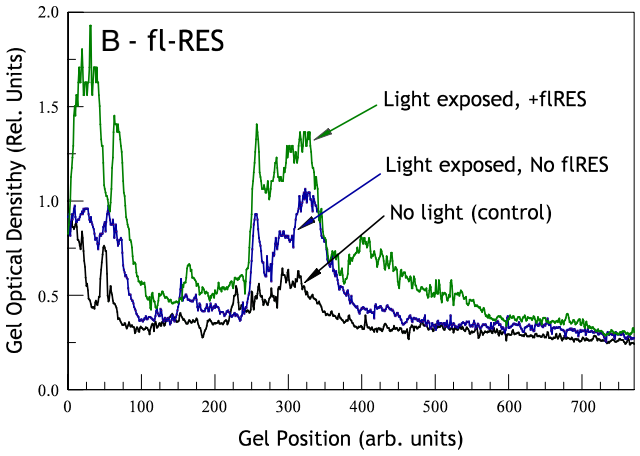

Figure 5. Protein carbonylation in RPE cells exposed to the output of the Hg vapor arc lamp (10 min at 19 mW cm^{-2}). RES treatment decreased the number of carbonyl adducts below that found in the control (untreated and unexposed) cells, whereas fl-RES increased oxidation of virtually all of the proteins resolved in the gel. The figures show optical density scans of the images of Western blots resulting from the Oxyblot assay of protein carbonyl adducts in the cells following a 24 h incubation at 37°C after the light exposure (further details are given in the Materials and Methods section). The area under these traces was integrated and used as a quantitative measure to compare the carbonyl loads in each treatment group (see Table 1 for a summary of these data). (A) Effect of RES pretreatment. Explanation of traces (top to bottom): "Light exposed, no RES" shows the level of protein carbonyls found in proteins in RPE cells that were exposed to light without RES pretreatment; "No light, no RES" is the protein carbonyl level in control cells neither light-exposed nor treated with RES; and "Light, +10 μM RES pretreatment" shows the protein carbonyl level in cells exposed to light after pretreatment with 10 μM RES. (B) Effect of fl-RES pretreatment (fl-RES concentration not determined, see text). Explanation of traces (top to bottom): "Light exposed, +flRES" shows protein carbonylation in cells pretreated with the fl-RES photoderivative and then exposed to light; "Light exposed, No flRES" shows protein carbonylation in cells exposed to light but not treated with fl-RES; and "No light (control)" shows protein carbonylation in control cells that did not receive light exposure or treatment with fl-RES.

to the upregulation of p53 in SM cells (Fig. 10B), which blocks cell cycling and proliferation, leading to an increase in apoptosis in SM cells treated with UA and exposed to UV–VIS. Thus, the effects of RES and UA are somewhat complementary: RES exerts general antioxidant effects (but see the next section for a discussion of its other actions, *e.g.* on

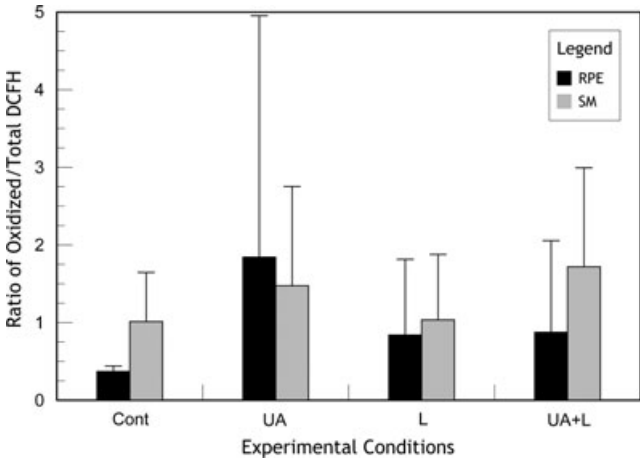

Figure 6. Reactive oxygen species in RPE and SM cells treated with UA. HPLC analysis of cells probed with the DCFH fluorescent indicator was used to assess oxidative stress in the cells under the various experimental conditions. The ordinate of the graph shows the proportion of DCFH oxidized in each group (n = 3 for RPE cells, and n = 2 for SM cells), which was determined by first measuring with HPLC the amount of oxidized DCFH in the treated cells, and then determining the total cellular content of DCFH in an aliquot of the cell lysate after chemically oxidizing all of the DCFH present, using horseradish peroxidase. Bars show the means and the error bars represent the ranges of experimentally determined values. Description of experimental conditions: Control = cells without any treatment; UA = cells treated with 2.2 μM UA; UA+L = cells treated with 2.2 μM UA and exposed to broadband light; L = cells treated with broadband light. In the groups exposed to light, the cells were irradiated at 26.7 mW cm^{-2} for 10 min.

the sirtuins), whereas UA appears to block cell cycle propagation, increase apoptosis and modulate—through its interactions with NF-κB signaling—some aspects of the cellular response to oxidative stress. Thus, the selective use of these phytochemicals may be useful in a variety of therapeutic applications.

Antioxidant effect of RES

Native RES, *i.e.* t-RES, at a low micromolar concentration, exerts a variety of antioxidant actions. This effect is typified by the reduction of protein carbonyls produced by photochemical damage (cf. Fig. 5A). The other salient finding is that the activation of NF-κB is reduced by RES pretreatment, suggesting a possible anti-inflammatory action of this phytochemical in ocular tissue. RES has been reported to exert anti-inflammatory effects in other tissue systems. For example, RES inhibits COX-2, a member of the family of cyclooxygenase enzymes, which plays a critical role in mediating inflammatory responses. RES has demonstrated anti-inflammatory activity in a number of model systems, such as LPS or other chemical and toxin-induced inflammatory responses (49–51), and ischemia-reperfusion (17). RES has also been found to modulate or reduce cell-signaling pathways, such as NF-κB and AP-1, both of which are involved in mediating inflammatory responses (52).

RES, and other plant polyphenols, may also confer protection through an entirely different pathway, *i.e.* by enhancing the activity of the SIRT1 or other sirtuin genes. This gene family increases gene stability by deacetylating histones and many other proteins in a variety of cell-signaling pathways,

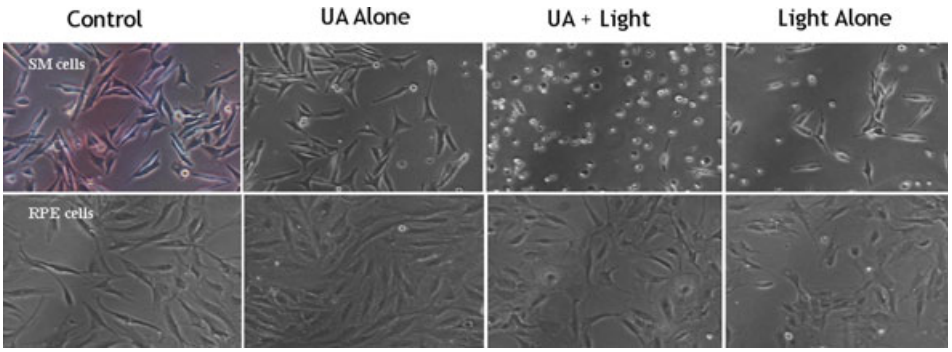

Figure 7. Morphological comparison of skin melanoma (SM) cells and RPE cells, 24 h after treatment with UA and UV–VIS radiation. Cells were treated with ursolic acid (2.2 μM) for 24 h prior to UV–VIS irradiation. After 24 h or postexposure incubation, the cells were imaged. The photomicrographs in the upper and the lower rows represent the morphological appearance of SM and RPE cells under four experimental conditions, respectively. Description of experimental conditions from left to right: Control = cells without any treatment; UA Alone = cells treated with UA only; UA + Light = cells treated with UA and broadband light exposure; Light Alone = cells exposed to broadband light without UA treatment. The cells were irradiated at an intensity of 26.7 mW cm^{-2} for 10 min.

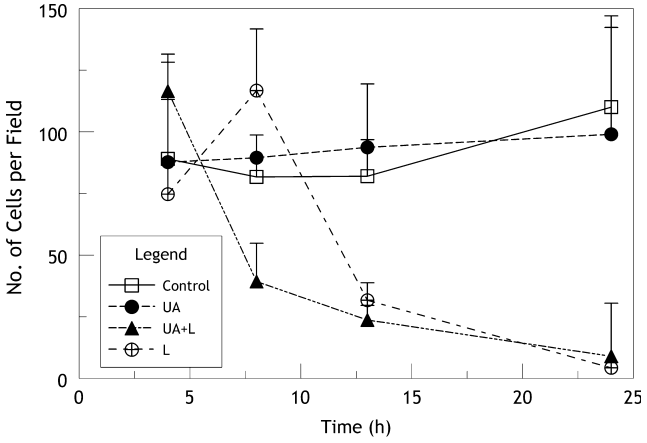

Figure 8. Cell proliferation in SM cells treated with UA and UV radiation. Cell growth was assessed by the average number of cells counted in three independent microscope fields over the designated time. The cells were imaged using phase contrast microscopy and the number of cells per field was counted manually. Legend: Control = cells without any treatment; UA = cells treated with 2.2 μM UA only; UA + L = cells treated with 2.2 μM UA and UV–VIS light exposure; L = cells exposed to UV–VIS light only. Light exposure conditions were as described in Fig. 7.

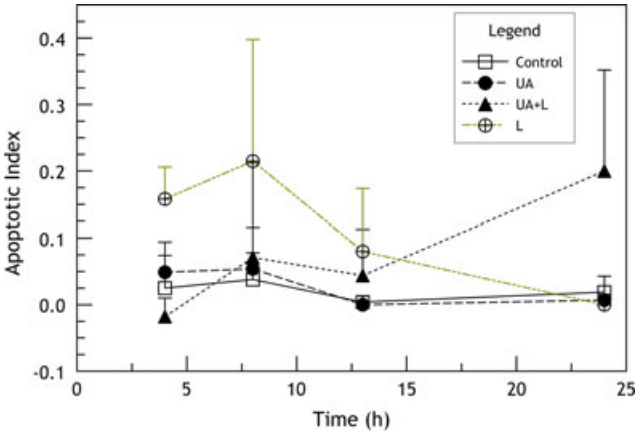

Figure 9. Proportion of apoptotic cells in each treatment group over time, as determined with the Vybrant YO-PRO-1 assay. This assay was performed using the Vybrant 4 live/dead cell assay, 4 h following the treatment of SM cells with UA (2.2 μM) and/or light exposure. Dead cells (*i.e.* necrotic) are initially permeable to the PI fluorescent probe only, whereas apoptotic cells only admit YO-PRO into the nuclei. Apoptosis in the figure is expressed mathematically by the apoptosis index (AI) as: $AI = [(h - Y)/(h - P)] - 1$, where h is the total number of cells, Y denotes the number of YO-PRO stained cells and P denotes the number of PI stained cells in the same field. Error bars in the figure represent the standard deviation values for each condition ($n = 3$). Legend: Control = cells without any treatment; UA = cells treated with 2.2 μM UA only; UA + L = cells treated with 2.2 μM UA and UV–VIS light exposure; L = cells exposed to UV–VIS light only. Light exposure conditions were as described in Fig. 7.

one result of which is increased lifespan (53). The action of plant polyphenols, such as RES, increases the affinity of SIRT1 for its substrates (53). In terms of ocular protection, activation of SIRT1 by intraocular injection of RES or synthetic pharmaceutical agents reduced the apoptotic loss of retinal cells in animal models of experimental uveitis (54,55). Other signaling pathways are beneficially modulated by RES, including signaling mediated by proinflammatory cytokines in cells of the trabecular meshwork in a glaucoma model (56), and CaM kinase II in retinal cells in a diabetes model (57). Thus, the ability to regulate signaling pathways is likely to be critical in the ability of this phytochemical to regulate inflammatory and immune responses *in vivo*.

Photosensitization by RES photoderivatives

The finding in this study that the RES photoderivative, fl-RES, can function as a photosensitizer, at least in promoting oxidative damage to proteins (Fig. 5), is of considerable relevance to the safe and effective use of RES as a nutritional supplement. It is well known that photodegradation of RES readily occurs upon exposure to natural or artificial light sources, *e.g.* red wine is packaged in green or brown glass bottles to shield out the shorter wavelengths that would degrade the quality of the product; however, if a sufficient quantity of the fl-RES end product is produced, then a potential health hazard may exist. This possibility must also be considered in the design of animal nutritional supplementation experiments, during which animal chow containing RES might be exposed for considerable lengths of time to standard laboratory fluorescent lighting, resulting in the conversion of

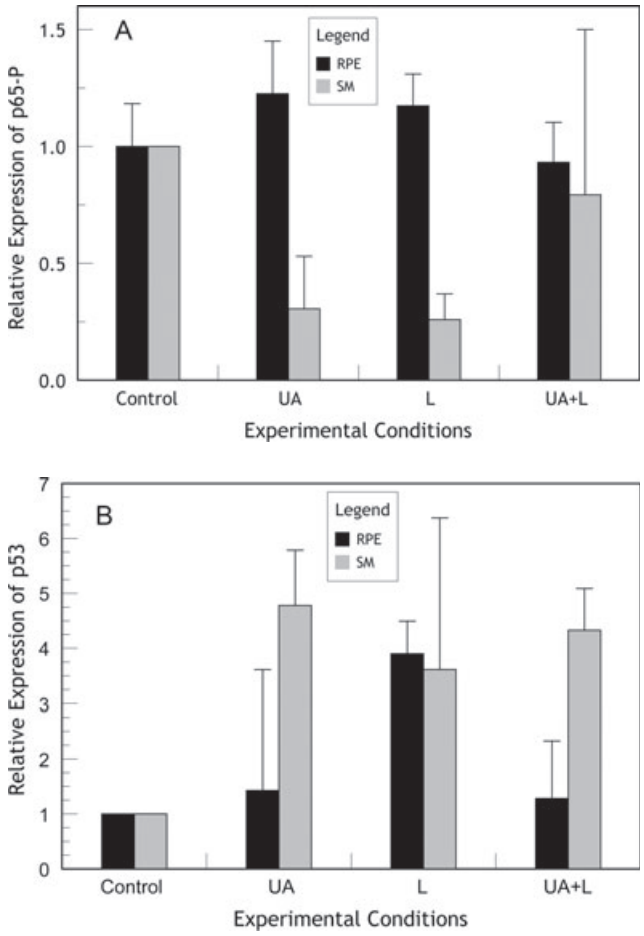

Figure 10. Protein expression in RPE and SM cells after UA treatment and UV–VIS exposure. Expression of NF-κB (p65-P) and p53 were determined by immunoprecipitation and Western blot analysis. (A) Total p65-P in response to the treatment of RPE and SM cells with UA and/or UV–VIS light. (B) Nuclear p53 upregulation in response to the treatment of UA and/or UV–VIS light. Bars indicate the mean values, and the error bars represent the ranges of experimentally determined values in the groups between each run (n = 2 for all measurements). Description of experimental conditions: Control = cells without any treatment; UA = cells treated with 2.2 μM UA only; UA + L = cells treated with 2.2 μM UA and UV–VIS light; L = cells exposed to UV–VIS light only. Light exposure conditions were as described in Fig. 7.

some of the compound to fl-RES. Even if the amount of fl-RES produced is insufficient by itself to produce photosensitized reactions in the animals, the loss of RES due to photoderivatization will result in a lower RES intake for the animals. Fortunately, the pellet matrix of some laboratory animal chows may shield the RES from excessive light exposure; our group has found that RES formulated in AIN-93G mouse chow pellets was stable for at least 6 months (unpublished data). Nevertheless, RES may not be stable in all pellet formulations, and precautions should be taken to prevent excessive exposure of RES-supplemented animal chows to fluorescent or daylight sources.

Differential effects of UA in normal and tumor cells

Although the present data are inconclusive, UA treatment tended to increase the level of intracellular oxidative stress as measured by the extent of DCFH oxidation. This effect suggests that UA may be able to modify the underlying cellular metabolism, which is a potentially useful strategy for cancer therapy (58). Notably, SM cells maintained better homeostasis when confronted with elevated oxidative stress than did RPE cells upon radiation exposure, based on the result of the intracellular DCFH assay. The capacity of cells to withstand oxidative stress, however, was reported to be restored by UA, albeit at a higher concentration (IC_{50} = 140.76 μg mL^{-1}) (23) than was used in the present investigation. The importance of the UA-induced increase in ROS may be that it triggers markedly different intracellular signaling patterns found between normal and cancer cells following UV radiation. Upon treatment with UA at micromolar concentrations, the resulting levels of p53 expression and NF-κB activation were very different in the RPE and SM cell lines, strongly implicating a specific modulatory effect of UA. The stimulatory effect on p53 expression and the inhibitory effect on NF-κB activation exerted by UA preferentially occurred in SM cells. The differential activation of these two signaling pathways, combined with the observed radiation killing effect through apoptosis, supports the conclusion that UA sensitizes SM cells to UV radiation while protecting RPE cells from radiation damage. Preliminary data suggest that similar actions of UA are also found in these cells after exposure to gamma radiation. Considering its low toxicity to normal cells, and common occurrence in the human diet, UA may be a promising candidate for inclusion in clinical radiotherapeutic protocols to increase the radiosensitivity of tumor cells while simultaneously providing some degree of radioprotection to normal cells.

Practical considerations in the use of nutraceuticals to achieve therapeutic endpoints

In our studies, as well as most of those in the literature, the observed therapeutic endpoints have been achieved at concentrations of the agent in the range of 1–10 μM. The bioavailability of these agents *in vivo*, however, is generally limited, and typically much lower systemic levels are achieved by oral intake. For example, the serum levels of RES in mice required to obtain some of the pharmacological effects reported have been as high as 1500 mg kg^{-1} (9)—practically impossible to achieve by feeding alone. In humans, the safe intakes of RES from sources such as wine are limited, so that even including the circulating amounts of RES metabolites, an upper effective concentration of about 2 μM might be achieved by dietary sources (9) (although the sulphonated and glucuronide metabolites probably have little bioactivity). Similarly, the few pharmacokinetic investigations of UA have found low systemic uptake. For example, in rats after gavage feeding of large amounts of the compound, serum UA reached a peak concentration of approximately 300 ng mL^{-1} (0.66 μM) (59). There is no information on the ocular pharmacokinetics of these compounds, but it is likely that much lower levels reach the retina and RPE from the serum. We do not yet have information on the cellular uptake or retention of these compounds. Therefore, the obstacle of low ocular bioavailability of RES and UA, along with limited pharmacokinetic data, must be overcome before these compounds can be used to achieve predictable therapeutic effects in the eye. This may

be achieved by the synthesis of chemical derivatives with superior systemic uptake and distribution, a route currently being explored commercially. Until such agents are available, it is likely that regular nutritional intake of these compounds will be the most practical way to obtain whatever beneficial effect on ocular health is conferred by the low systemic concentrations achieved *via* dietary sources.

Acknowledgements—This work has been supported in part by the RMG Research Endowment, a grant from the Julio Palmaz Endowment in the Department of Radiology at the UTHSCSA (Y-HL) and a grant from the University of Texas System/San Antonio Life Sciences Institute (RDG). Y-HL was supported by National Science Foundation Partnerships for Research and Education in Materials (PREM) Grant No. DMR-0934218 in collaboration with Northwestern University MRSEC.

REFERENCES

1. Hillenkamp, F. (1989) Laser radiation tissue interaction. *Health Phys*. **56**, 613–616.
2. Jacques, S. L. (1997) Laser-tissue interactions. In *Non-Ionizing Radiation: An Overview of the Physics and Biology* (Edited by K. Hardy, M. Meltz and R. D. Glickman), pp. 81–98. Medical Physics Publishing, Madison,WI.
3. Glickman, R. D. (2002) Phototoxicity to the retina: Mechanisms of damage. *Int. J. Toxicol*. **21**, 473–490.
4. Sliney, D. H. (2005) Exposure geometry and spectral environment determine photobiological effects on the human eye. *Photochem. Photobiol*. **81**, 483–489.
5. Taylor, H. R., B. Munos, S. West, N. M. Bressler, S. B. Bressler and F. S. Rosenthal (1990) Visible light and risk of age-related macular degeneration. *Trans. Am. Ophthalmol. Soc*. **88**, 163–178.
6. Tomany, S. C., K. J. Cruickshanks, R. Klein, B. E. Klein and M. D. Knudtson (2004) Sunlight and the 10-year incidence of age-related maculopathy: The Beaver Dam Eye Study. *Arch. Ophthalmol*. **122**, 750–757.
7. Cabrera, M. P. and R. H. Chihuailaf (2011) Antioxidants and the integrity of ocular tissues. *Vet. Med. Int*. **2011**, 905153 (pp. 1–8).
8. Kelsey, N. A., H. M. Wilkins and D. A. Linseman (2010) Nutraceutical antioxidants as novel neuroprotective agents. *Molecules* **15**, 7792–7814.
9. Baur, J. A. and D. A. Sinclair (2006) Therapeutic potential of resveratrol: The in vivo evidence. *Nat. Rev. Drug Discov*. **5**, 493–506.
10. Das, D. K. and N. Maulik (2006) Resveratrol in cardioprotection: A therapeutic promise of alternative medicine. *Mol. Interv*. **6**, 36–47.
11. Gehm, B. D., J. M. McAndrews, P. Y. Chien and J. L. Jameson (1997) Resveratrol, a polyphenolic compound found in grapes and wine, is an agonist for the estrogen receptor. *Proc. Natl Acad. Sci. USA* **94**, 14138–14143.
12. Klinge, C. M., K. E. Risinger, M. B. Watts, V. Beck, R. Eder and A. Jungbauer (2003) Estrogenic activity in white and red wine extracts. *J. Agric. Food Chem*. **51**, 1850–1857.
13. Turner, R. T., G. L. Evans, M. Zhang, A. Maran and J. D. Sibonga (1999) Is resveratrol an estrogen agonist in growing rats? *Endocrinology* **140**, 50–54.
14. Basly, J. P., F. Marre-Fournier, J. C. Le Bail, G. Habrioux and A. J Chulia (2000) Estrogenic/antiestrogenic and scavenging properties of (E)- and (Z)-resveratrol. *Life Sci*. **66**, 769–777.
15. Sato, M., G. Maulik, D. Bagchi and D. K. Das (2000) Myocardial protection by protykin, a novel extract of trans-resveratrol and emodin. *Free Radic. Res*. **32**, 135–144.
16. Sato, M., P. S. Ray, G. Maulik, N. Maulik, R. M. Engelman, A. A. Bertelli, A. Bertelliand and D. K. Das (2000) Myocardial protection with red wine extract. *J. Cardiovasc. Pharmacol*. **35**, 263–268.
17. Shigematsu, S., S. Ishida, M. Hara, N. Takahashi, H. Yoshimatsu, T. Sakata and R. J. Korthuis (2003) Resveratrol, a red wine constituent polyphenol, prevents superoxide-dependent inflammatory responses induced by ischemia/reperfusion, platelet-activating factor, or oxidants. *Free Radic. Biol. Med*. **34**, 810–817.
18. Losa, G. A. (2003) Resveratrol modulates apoptosis and oxidation in human blood mononuclear cells. *Eur. J. Clin. Invest*. **33**, 818–823.
19. Yen, G. C., P. D. Duh and C. W. Lin (2003) Effects of resveratrol and 4-hexylresorcinol on hydrogen peroxide-induced oxidative DNA damage in human lymphocytes. *Free Radic. Res*. **37**, 509–514.
20. Ahmad, A., F. A. Syed, S. Singh and S. M. Hadi (2005) Prooxidant activity of resveratrol in the presence of copper ions: Mutagenicity in plasmid DNA. *Toxicol. Lett*. **159**, 1–12.
21. Gatz, S. A. and L. Wiesmuller (2008) Take a break—Resveratrol in action on DNA. *Carcinogenesis* **29**, 321–332.
22. Roemer, K. and M. Mahyar-Roemer (2002) The basis for the chemopreventive action of resveratrol. *Drugs Today (Barc)* **38**, 571–580.
23. Ali, M. S., S. A. Ibrahim, S. Jalil and M. I. Choudhary (2007) Ursolic acid: A potent inhibitor of superoxides produced in the cellular system. *Phytother. Res*. **21**, 558–561.
24. Najid, A., A. Simon, J. Cook, H. Chable-Rabinovitch, C. Delage, A. J. Chulia and M. Rigaud (1992) Characterization of ursolic acid as a lipoxygenase and cyclooxygenase inhibitor using macrophages, platelets and differentiated HL60 leukemic cells. *FEBS Lett*. **299**, 213–217.
25. Yin, M. C. and K. C. Chan (2007) Nonenzymatic antioxidative and antiglycative effects of oleanolic acid and ursolic acid. *J. Agric. Food Chem*. **55**, 7177–7181.
26. Balanehru, S. and B. Nagarajan (1991) Protective effect of oleanolic acid and ursolic acid against lipid peroxidation. *Biochem. Int*. **24**, 981–990.
27. Shishodia, S., S. Majumdar, S. Banerjee and B. B. Aggarwal (2003) Ursolic acid inhibits nuclear factor-kappaB activation induced by carcinogenic agents through suppression of IkappaB-alpha kinase and p65 phosphorylation: Correlation with down-regulation of cyclooxygenase 2, matrix metalloproteinase 9, and cyclin D1. *Cancer Res*. **63**, 4375–4383.
28. Mohan, S., K. Koyoma, A. Thangasamy, H. Nakano, R. D. Glickman and N. Mohan (2007) Low shear stress preferentially enhances IKK activity through selective sources of ROS for persistent activation of NF-kappaB in endothelial cells. *Am. J. Physiol. Cell Physiol*. **292**, C362–C371.
29. Pahl, H. L. (1999) Activators and target genes of Rel/NF-kappaB transcription factors. *Oncogene* **18**, 6853–6866.
30. Raju, U., G. J. Gumin and P. J. Tofilon (2000) Radiation-induced transcription factor activation in the rat cerebral cortex. *Int. J. Radiat. Biol*. **76**, 1045–1053.
31. Vile, G. F., A. Tanew-Ilitschew and R. M. Tyrrell (1995) Activation of NF-kappa B in human skin fibroblasts by the oxidative stress generated by UVA radiation. *Photochem. Photobiol*. **62**, 463–468.
32. Li, N. and M. Karin (1998) Ionizing radiation and short wavelength UV activate NF-kappaB through two distinct mechanisms. *Proc. Natl Acad. Sci. USA* **95**, 13012–13017.
33. Glickman, R. D., M. Natarajan, B. A. Rockwell, M. Denton, S. Maswadi, N. Kumar and F. Nieves-Roldan (2005) Intracellular signaling mechanisms responsive to laser-induced photochemical and thermal stress. In *Optical Interactions with Tissue and Cells XVI* (Edited by S. L. Jacques and W. P. Roach), *Proc. SPIE* **5695**, 260–269.
34. Legrand-Poels, S., S. Schoonbroodt, J. Y. Matroule and J. Piette (1998) NF-kappa B: An important transcription factor in photobiology. *J. Photochem. Photobiol. B, Biol* **45**, 1–8.
35. Yim, E. K., K. H. Lee, S. E. Namkoong, S. J. Um and J. S. Park (2006) Proteomic analysis of ursolic acid-induced apoptosis in cervical carcinoma cells. *Cancer Lett*. **235**, 209–220.
36. Yim, E. K., M. J. Lee, K. H. Lee, S. J. Um and J. S. Park (2006) Antiproliferative and antiviral mechanisms of ursolic acid and dexamethasone in cervical carcinoma cell lines. *Int. J. Gynecol. Cancer* **16**, 2023–2031.
37. Huang, M. T., C. T. Ho, Z. Y. Wang, T. Ferraro, Y. R. Lou, K. Stauber, W. Ma, C. Georgiadis, J. D. Laskin and A. H. Conney (1994) Inhibition of skin tumorigenesis by rosemary and its constituents carnosol and ursolic acid. *Cancer Res*. **54**, 701–708.
38. Tokuda, H., H. Ohigashi, K. Koshimizu and Y. Ito (1986) Inhibitory effects of ursolic and oleanolic acid on skin tumor

promotion by 12-O-tetradecanoylphorbol-13-acetate. *Cancer Lett*. **33**, 279–285.
39. De Angel, R. E., S. M. Smith, R. D. Glickman, S. N. Perkins and S. D. Hursting (2010) Antitumor effects of ursolic acid in a mouse model of postmenopausal breast cancer. *Nutr. Cancer* **62**, 1074–1086.
40. Trela, B. C. and A. L. Waterhouse (1996) Resveratrol: Isomeric molar absorptivities and stability. *J. Agric. Food Chem*. **44**, 1253–1257.
41. Jayatilake, G. S., H. Jayasuriya, E. S. Lee, N. M. Koonchanok, R. L. Geahlen, C. L. Ashendel, J. L. McLaughlin and C. J. Chang (1993) Kinase inhibitors from Polygonum cuspidatum. *J. Nat. Prod*. **56**, 1805–1810.
42. Galeano-Diaz, T., I. Duran-Meras and D. Airado-Rodriguez (2007) Isocratic chromatography of resveratrol and piceid after previous generation of fluorescent photoproducts: Wine analysis without sample preparation. *J. Sep. Sci*. **30**, 3110–3119.
43. Dontsov, A. E., R. D. Glickman and M. A. Ostrovsky (1999) Retinal pigment epithelium pigment granules stimulate the photooxidation of unsaturated fatty acids. *Free Radic. Biol. Med*. **26**, 1436–1446.
44. Rambhatla, L., C. P. Chiu, R. D. Glickman and C. Rowe-Rendleman (2002) In vitro differentiation capacity of telomerase immortalized human RPE cells. *Invest. Ophthalmol. Visual. Sci*. **43**, 1622–1630.
45. Natarajan, M., B. K. Nayak, C. Galindo, S. P. Mathur, F. N. Roldan and M. L. Meltz (2006) Nuclear translocation and DNA-binding activity of NFKB (NF-kappaB) after exposure of human monocytes to pulsed ultra-wideband electromagnetic fields (1 kV/cm) fails to transactivate kappaB-dependent gene expression. *Radiat. Res*. **165**, 645–654.
46. Glickman, R. D., M. Vendal, M. A. Gonzales and N. Kumar (1999) Intracellular photochemical reactions in the RPE cell exhibit a wavelength dependence that resembles the action spectrum of melanin. In *Laser-Tissue Interaction X: Photochemical, Photothermal, and Photomechanical* (Edited by S. L. Jacques), *Proc. SPIE* **3601**, 94–101.
47. Glickman, R. D. (2011) Ultraviolet phototoxicity to the retina. *Eye Contact Lens* **37**, 196–205.
48. Mainster, M. A. and P. L. Turner (2010) Ultraviolet-B phototoxicity and hypothetical photomelanomagenesis: Intraocular and crystalline lens photoprotection. *Am. J. Ophthalmol*. **149**, 543–549.
49. Birrell, M. A., K. McCluskie, S. Wong, L. E. Donnelly, P. J. Barnes and M. G. Belvisi (2005) Resveratrol, an extract of red wine, inhibits lipopolysaccharide induced airway neutrophilia and inflammatory mediators through an NF-kappaB-independent mechanism. *FASEB J*. **19**, 840–841.
50. Chen, G., W. Shan, Y. Wu, L. Ren, J. Dong and Z. Ji (2005) Synthesis and anti-inflammatory activity of resveratrol analogs. *Chem. Pharm. Bull. (Tokyo)* **53**, 1587–1590.
51. Elmali, N., I. Esenkaya, A. Harma, K. Ertem, Y. Turkoz and B. Mizrak (2005) Effect of resveratrol in experimental osteoarthritis in rabbits. *Inflamm. Res*. **54**, 158–162.
52. Rahman, I., S. K. Biswas and P. A. Kirkham (2006) Regulation of inflammation and redox signaling by dietary polyphenols. *Biochem. Pharmacol*. **72**, 1439–1452.
53. Porcu, M. and A. Chiarugi (2005) The emerging therapeutic potential of sirtuin-interacting drugs: From cell death to lifespan extension. *Trends Pharmacol. Sci*. **26**, 94–103.
54. Anekonda, T. S. and G. Adamus (2008) Resveratrol prevents antibody-induced apoptotic death of retinal cells through upregulation of Sirt1 and Ku70. *BMC Res. Notes* **1**, 122.
55. Shindler, K. S., E. Ventura, T. S. Rex, P. Elliott and A. Rostami (2007) SIRT1 activation confers neuroprotection in experimental optic neuritis. *Invest. Ophthalmol. Vis. Sci*. **48**, 3602–3609.
56. Luna, C., G. Li, P. B. Liton, J. Qiu, D. L. Epstein, P. Challa and P. Gonzalez (2009) Resveratrol prevents the expression of glaucoma markers induced by chronic oxidative stress in trabecular meshwork cells. *Food Chem. Toxicol*. **47**, 198–204.
57. Kim, Y. H., Y. S. Kim, S. S. Kang, G. J. Cho and W. S. Choi (2010) Resveratrol inhibits neuronal apoptosis and elevated Ca^{2+}/calmodulin-dependent protein kinase II activity in diabetic mouse retina. *Diabetes* **59**, 1825–1835.
58. Baffy, G., Z. Derdak and S. C. Robson (2011) Mitochondrial recoupling: A novel therapeutic strategy for cancer? *Br. J. Cancer* **105**, 469–474.
59. Liao, Q., W. Yang, Y. Jia, X. Chen, Q. Gao and K. Bi (2005) LC-MS determination and pharmacokinetic studies of ursolic acid in rat plasma after administration of the traditional Chinese medicinal preparation Lu-Ying extract. *Yakugaku Zasshi* **125**, 509–515.